Are cosmic rays affecting high-latitude winter cyclones?

Jake Hebert

Because of their belief that 'the present is the key to the past', uniformitarian climatologists have become convinced that past dramatic fluctuations in climate can also occur in the present. Within the creation model, however, these dramatic climate fluctuations occurred during a single Ice Age that followed the (non-repeatable) Genesis Flood. Hence, in the creation model, these past climate fluctuations cannot legitimately be used to extrapolate future climate changes. Hence there is a subtle connection between denial of the Genesis Flood and anxiety over 'climate change'. A better understanding of cloud microphysics would also be helpful in gaining greater clarity on this issue. It is possible that current meteorological and climatological models are not taking into account all the relevant physics. In recent years there has been considerable interest in theories that cosmic rays could influence weather and climate. The best-publicized mechanism for such a link is Henrik Svenmsark's theory of 'ion-mediated nucleation' (IMN). A second, less well-known mechanism, called 'charge modulation of aerosol scavenging' (CMAS), involves the downward 'fair-weather' ionosphere-to-surface electric current density J_z. A prediction of the CMAS mechanism is that increases in J_z will intensify high-latitude northern hemisphere winter cyclones. Evidence for such an effect is presented from two independent data sets.

Uniformitarian interpretations of earth history are helping to 'fuel' alarmism over 'climate change' or 'global warming'.[1] Both creation and uniformitarian scientists think fluctuations in $\delta^{18}O$ levels within the high-latitude ice sheets are suggestive of past dramatic temperature fluctuations (possibly as high as 20°C).[2] Creation scientists argue that these fluctuations occurred during a single Ice Age following the (non-repeatable) Genesis Flood. Hence, in the creation model, such past climate fluctuations cannot legitimately be used to predict possible future climatic changes. Because of their belief that 'the present is the key to the past', uniformitarian scientists believe such sudden temperature changes may occur in the future, and that the consequences of such changes could be disastrous.

Hence there is a subtle connection between the creation–evolution issue and anxiety over 'global warming'. Thus a biblical worldview helps to guard against alarmism in this area.

Another reason for taking a judicious approach toward this issue is 'gaps' in our understanding of meteorology: there is a very real possibility that current meteorological and climatological models are not taking into account all the relevant physics. In particular, there is a possibility that cosmic rays could be influencing weather and climate.

Currently, there are two major proposed theoretical mechanisms linking cosmic rays to weather and climate.[3] Both mechanisms involve the fact that increased cosmic ray (mainly proton) fluxes into the atmosphere will increase the number of atmospheric ions. The first mechanism is called *ion-mediated nucleation* (IMN) and has been researched by Danish physicist Henrik Svensmark. The second mechanism, *charge modulation of aerosol scavenging* (CMAS) has been researched by Brian Tinsley[4] of the University of Texas at Dallas and has been discussed in two previous papers.[5,6] An effect predicted by the CMAS theory (but not by the IMN theory) is that increases in the downward 'fair-weather' ionosphere-to-surface electric current density J_z will intensify high-latitude northern hemisphere winter cyclones.

Summary of the CMAS mechanism

A brief summary of the CMAS mechanism is included here. The ionosphere and surface of the earth may be thought of as conducting 'plates' of a spherically symmetric capacitor (figure 1). The ionosphere has a global electric potential V_i[7] that varies between 200 and 300 kV[8] (with an average value of ~250 kV) relative to the earth's surface.[9] This potential is maintained by upward transport of charge from a number of sources, the most important of which are low-latitude thunderstorm 'generators'.[10] Because the earth's atmosphere is a weak conductor of electricity, this potential difference drives a downward 'fair-weather' electric current of about

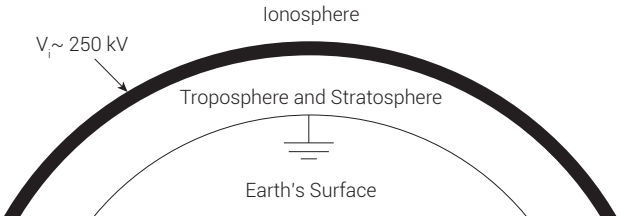

Figure 1. Simplified diagram showing how the ionosphere and surface of the earth may be viewed as conducting plates of a 'leaky' spherically symmetric capacitor.

1 kiloampere.[11] The density J_z of this current is very tiny, about 1–6 trillionths of an ampere per square metre (pA/m^2).[12]

Because the atmosphere is very thin compared to the earth's radius, one may simplify calculations by treating the ionosphere and surface of the earth as 'plates' of a *parallel* plate capacitor. 'Sandwiched' between these two plates are the troposphere and stratosphere.

Because the resistivity of the atmosphere is dependent upon local ionisation rates and aerosol contents, the electrical resistance of a column of air between the earth's surface and the base of the ionosphere will vary from one location to another. The resistance of a column of air with a base of 1 square metre is called the *columnar resistance* (units of Ωm^2) and is denoted by R. This columnar resistance is composed of two resistors in series, the columnar resistance T of the troposphere and the columnar resistance S of the stratosphere (figure 2). Ohm's Law gives the relationship between J_z, V_i, T, and S:

$$J_z = \frac{V_i}{R} = \frac{V_i}{T+S} \quad (1)$$

Thus, changes in V_i, T, or S will affect J_z. For instance, *decreasing* cosmic rays into the troposphere will *decrease* the number of tropospheric ions, resulting in an *increase* in T. For a given ionospheric potential V_i, this will result in *lower* values of J_z.

Because clouds are much less electrically conducting than the surrounding air,[13] conductivity gradients will exist at the tops and bottoms of clouds. One may use Ohm's and Gauss's Laws to show that J_z will result in the presence of electric charge at these cloud boundaries (figure 3):

$$\rho(z) = \left[\frac{\varepsilon_O}{\sigma^2}\frac{\partial\sigma}{\partial z}\right] J_z \quad (2)$$

Here ρ is electric charge density, ε_O is a constant called the *permittivity of free space*, and σ is the electrical conductivity. Eq. 2 shows that this charge will be present

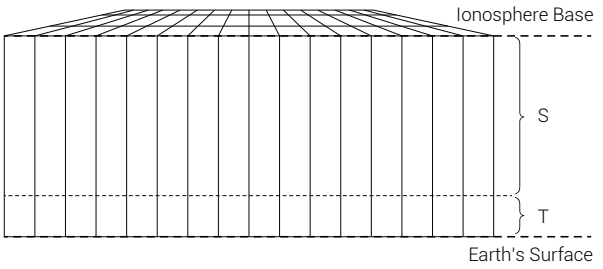

Figure 2. Because the thickness of the atmosphere is negligible compared to the earth's radius, one may simplify calculations by modelling the ionosphere and surface of the earth as conducting plates of a parallel capacitor, between which are 'sandwiched' the troposphere and stratosphere. The lower atmosphere is composed of many columnar resistances in parallel with each other, each of which is composed of a tropospheric columnar resistance in series with a stratospheric columnar resistance (after figure 1.2 in Hebert[37]).

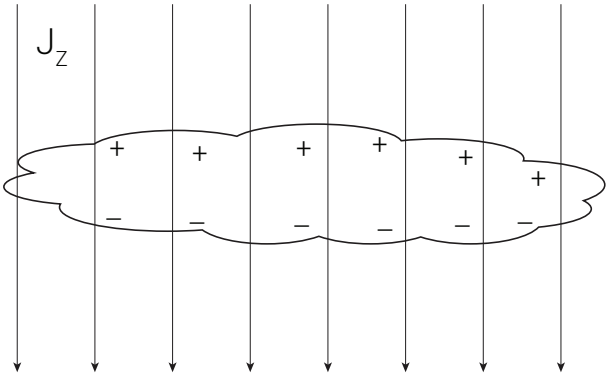

Figure 3. Charge will be present at locations where J_z passes through gradients in conductivity (or resistivity), such as are present at cloud boundaries. This charge will become attached to cloud droplets and aerosols, modulating the rates at which aerosols are scavenged by the droplets. Since some of these aerosols may act as cloud-condensation or ice-forming nuclei, this 'charge modulation of aerosol scavenging' (CMAS) can conceivably affect precipitation and cloud lifetimes.

at places where the electrical conductivity changes with height *z*. It also shows that increases in J_z will increase this charge density, and decreases in J_z will decrease this charge density.

The conductivity gradient will be negative as one enters the cloud from below, resulting in a layer of negative charge at the lower cloud boundary. Likewise, because the conductivity gradient is positive as one exits the cloud top, a layer of positive charge will be present at the upper cloud boundary.

This charge will be found on cloud droplets, as well as on aerosols within the clouds. Thus aerosols and water droplets at cloud tops will tend to have the same sign, as will aerosols and droplets at cloud bottoms.

One might naively suspect that these 'like charges' would simply cause the aerosols and droplets to be repelled from one another (since 'like' charges repel). However, the presence of conducting acids and salts in cloud condensation nuclei (CCNs) and cloud droplets means that both are actually tiny conducting spheres of varying size.[14,15] Because these spheres generate 'image' charges on one another, the resulting electrostatic force between a droplet and aerosol in a weakly electrified cloud involves a long-range repulsive force and two short-range attractive forces.[16]

Determining the trajectory of an aerosol relative to a cloud droplet is quite complicated, due to the numerous forces acting upon it, as well as the random collisions ('Brownian motion') between the aerosol and other particles. Thus, Monte Carlo computer simulations must be used to determine the effect that such random collisions have upon the aerosol trajectories.

These simulations have shown that for aerosols and droplets of the same sign the CMAS effect tends to increase the rates at which large aerosols (radius $>\sim 0.1$ μm) are scavenged by cloud droplets, while simultaneously reducing the rates at which smaller aerosols are scavenged.[17] This effect upon the droplet size distribution within the cloud has been discussed in a previous paper.[5]

Another prediction of Tinsley's CMAS effect is that intensities of northern hemisphere high-latitude winter cyclones should increase when J_z increases and decrease when J_z decreases. The rationale for this prediction is given below.

Intensification of northern hemisphere high-latitude winter cyclones

Before explaining how variations in J_z could affect cyclonic intensity, it is necessary to review some background information. A *Forbush decrease* is a sudden, short-term decrease in galactic cosmic ray (GCR) flux into the atmosphere. A Forbush decrease occurs when a large bubble of plasma (known as a *coronal mass ejection*) that has been ejected from the Sun reaches Earth. Likewise, a *heliospheric current sheet* (HCS) *crossing* is the passing of the earth through a wavy layer of electrical current (the *heliospheric current sheet*) that separates the magnetic field lines from one solar hemisphere from the field lines from the other solar hemisphere. These magnetic field lines extend into, and are 'frozen into', the solar wind plasma (figures 4 and 5).

Intensities of northern hemisphere extended winter (November–March) cyclones have been observed to decrease at times of Forbush decreases,[18] as well as at times of HCS crossings (but for HCS crossings, these decreases only occur during times of high stratospheric aerosol content).[19] Specifically, decreases in a quantity called the *vorticity area index* (VAI) were observed (discussed below). During Forbush decreases, values of J_z decrease, via eq. 1. Likewise, values of J_z also decrease during HCS crossings, but only during periods of high stratospheric aerosol loading (changes in S should only affect J_z when S is comparable to T; i.e. during periods of high stratospheric aerosol loading[20]). Thus, we see that decreases in J_z are associated with decreases in northern hemisphere winter cyclonic intensity. Could the decreases in J_z be *causing* these decreases in cyclonic intensity? If so, one would also expect *increases* in J_z to cause *increases* in cyclonic intensity. The following is Tinsley's explanation of the possible link between J_z and cyclonic intensity (vorticity).[21]

Higher values of J_z cause more charge to be present on aerosols and droplets within a cloud, via eq. 2. Computer simulations have shown that the presence of greater amounts of charge causes an increase in the rate at which large

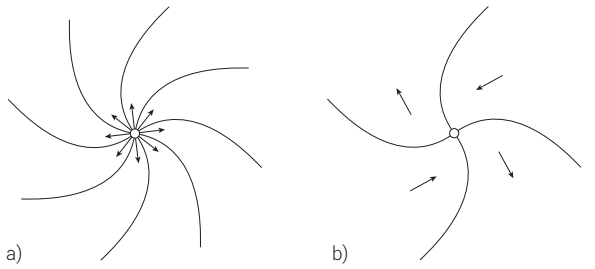

Figure 4. a) The radially outward motion of the solar wind (indicated by arrows), the sun's rotation, and the 'freezing in' of magnetic field lines within the solar wind plasma result in a 'spiral' pattern for the interplanetary magnetic field (IMF) within the solar equatorial plane (after Holzer[41]). **b)** Fairly typical 4-sector structure for the IMF. Arrows indicate regions of inward and outward radial IMF components.

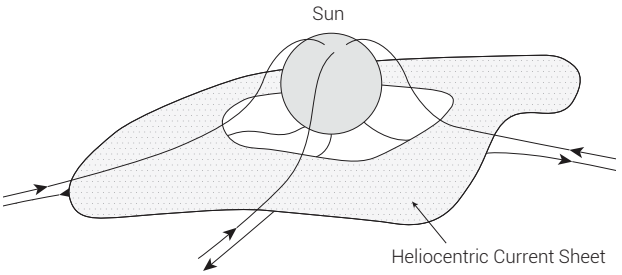

Figure 5. Simplified drawing depicting the 'ballerina' model of the heliospheric current sheet (the 'spiral' pattern of the field lines resulting from the 'garden hose' effect is not evident in this drawing) (after Smith[42]).

(>~0.1 μm radius) aerosols are scavenged by cloud droplets, with an accompanying simultaneous decrease in the rate at which small aerosols are scavenged.[17] This would likely result in greater ice formation through two different mechanisms.

First, because most ice-forming nuclei (IFNs) tend to have radii larger than ~0.1 μm,[22] the CMAS effect is expected to increase the numbers of IFNs scavenged by water droplets within clouds, including supercooled water droplets (droplets that are still liquid although they are below the freezing point of water). This would result in greater primary ice production from increased contact ice nucleation (the freezing of these supercooled droplets due to the presence of an IFN). Second, the CMAS effect tends to narrow the droplet size distribution within a cloud, with an accompanying decrease in average droplet size. This in turn results in a smaller likelihood of precipitation. Delayed precipitation makes it more likely that smaller droplets may be lifted by updrafts into the freezing level within a cloud *before* they can precipitate as rain.[23] Both of these mechanisms would result in the formation of additional ice within clouds in general and within cyclonic clouds in particular.

Increased ice production within a cyclone would then release additional latent heat of fusion, which would warm the air within the cyclone interior. Since warm air rises, this would enhance updraft vigor, resulting in a greater upward flow of air, provided that latent heat is a significant energy source for the updraft. This would especially be the case for 'baroclinic'[24] cyclones, such as high-latitude 'polar lows'. Polar lows in the northern hemisphere are most common during the winter months.[25]As this warmed air rises, it is 'replaced' by air from lower elevations; i.e. this increased upward flow of air within the cyclone interior will be accompanied by an inward flow of air from lower altitudes. Since air has mass, this inward flow of air results in more mass being brought closer to the cyclone's axis of rotation. Conservation of angular momentum then requires an increase in the cyclone's rotation speed. This is very similar to the manner in which a rotating figure skater spins faster when she pulls her arms and legs closer to her torso. This increased rotation speed results in an increase in a quantity called *vorticity*.

Vorticity

Air at a given location will have a given velocity (speed and direction). One can describe the overall pattern of air velocities with a *velocity field*. The velocity field assigns a speed and direction to every point. This velocity field may be represented visually by a collection of small arrows of varying lengths and directions. The length of an arrow at a given location is proportional to the speed of the air at that location, and the arrow's direction indicates the direction in which the air is moving.

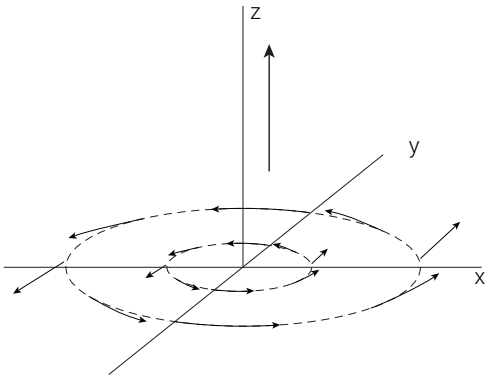

Figure 6. Diagram illustrating the curl of a two-dimensional velocity field. Because the velocity field 'rotates' in a counter-clockwise sense, the familiar 'right-hand rule' indicates that the curl points along the positive *z*-axis at every point in the *x*-*y* plane (after Griffiths[43]).

The *curl* of the velocity field is called *vorticity* and is a measure of how much the velocity 'curls' at a particular point.[26] In other words, it is a measure of microscopic rotation within a fluid (figure 6).[27] Roughly speaking, the individual 'curls' at various points can be 'added' together to get an overall measure of rotation within the fluid over a given area. In a cyclone or anticyclone, these individual 'curls' will combine to give an overall positive or negative number.[28] Because all northern hemisphere cyclones rotate counter-clockwise,[29] the familiar physics 'right-hand rule' indicates that they will all have positive vorticities (or more precisely, the local vertical components of their vorticities will be positive).

More rapidly rotating cyclones will be characterised by larger curls of their velocity fields, which yield higher values of their vertical vorticity components.

Greater high-latitude effect

Because of higher ionisation rates at high latitudes,[30] high-latitude columnar resistances will be smaller, resulting, via eq. 1, in higher average values of J_z. This then results, via eq. 2, in more average charge on aerosols and droplets within high-latitude cyclonic clouds. Thus, one might expect this intensification of cyclonic storms to be greatest at higher latitudes. VAI responses to inputs which modulate J_z have only been observed during the extended northern hemisphere winter,[18,19] and for this reason the analysis was restricted to data from the months of November–March. Since evidence of vorticity

modulation by J_z-modulating inputs only exists for the northern hemisphere, no attempt was made to verify such an effect for the southern hemisphere.[31]

The Vorticity Area Index (VAI)

The vorticity area index (VAI) is a standard measure of the strengths and areal extent of low pressure (cyclonic) systems. In essence, it is defined to be the surface area over which the vorticity (or more precisely, the vertical component of the vorticity) exceeds a threshold value.[32] This definition excludes, for the northern hemisphere, contributions from negative vorticities due to northern hemisphere high pressure (anticyclonic) systems. The VAI is calculated for a particular atmospheric pressure level and designated latitude band.

To test Tinsley's hypothesis, regressions of the VAI (or more precisely, changes in the VAI) were performed with J_z. The quantity ΔVAI for a given day was defined to be the difference between that day's average VAI value and the mean of the average VAI values for 15 days on either side. The CMAS theory predicts that ΔVAI should be positively correlated with high-latitude values of J_z.

Fair-weather values of J_z were measured at Mauna Loa Observatory (MLO) in Hawaii from 1960–1961[33] and 1977–1984 [34], but it is *local* values of J_z that are expected to modulate cyclone vorticity, and these J_z values can vary with location. Is there a way to 'connect' these MLO low-latitude J_z values with values of J_z at *higher* latitudes? Can the MLO J_z values legitimately 'stand in' for these higher-latitude J_z values?

A Proxy for high-latitude J_z

Yes, they can. Because the ionosphere is an excellent electrical conductor, the ionospheric electrical potential above an arbitrary low-latitude location will be *the same* as the electric potential above a high-latitude location.[34] If we take MLO to be our low-latitude location, Ohm's Law implies that

$$J_{z,high-lat} \times R_{high-lat} = J_{z,MLO} \times R_{MLO} \quad (3)$$

where 'high-lat' indicates a higher latitude than that of MLO. Dividing both sides of eq. 3 by $R_{high\text{-}lat}$ yields

$$J_{z,high-lat} = J_{z,MLO} \times \frac{R_{MLO}}{R_{high-lat}} \quad (4)$$

Hence, the higher-latitude J_z values which could be affecting high-latitude cyclonic intensity are proportional to the MLO J_z values, if the fraction in eq. 4 remains constant.

Of course, this fraction does not remain perfectly constant, as both the columnar resistances above MLO and at higher latitudes fluctuate due to local meteorological noise. Hence values of J_z measured at MLO are not a perfect proxy for these higher-latitude J_z values. However, they are arguably the best currently available proxy that can be used in such an analysis.

There are times when the fraction in eq. (4) changes significantly. The flux of galactic cosmic rays into the troposphere decreases during a Forbush decrease, resulting in a smaller number of tropospheric ions. Because the earth's magnetic field shields the lower latitudes from all but the most energetic particles, at such times higher latitudes experience a greater decrease in tropospheric ions than do lower latitudes. Hence high-latitude columnar resistances will experience greater percentage increases during a Forbush decrease than will low-latitude columnar resistances. Thus the fraction in eq. 4 at times of Forbush decreases can vary significantly from its value at other times, and MLO J_z values at such times may not serve as a proxy for higher-latitude J_z values. This difficulty may be circumvented by simply excluding from the analysis MLO J_z values that were measured during Forbush decreases.

There are uncertainties as to the manner in which high stratospheric aerosol loading affects the global electric circuit. Therefore, J_z values from winters a couple of years after the 1982 explosive eruption of the Mexican volcano El Chicón were also excluded from the analysis.

Mauna Loa J_z data

Other atmospheric electricity variables (such as positive and negative surface conductivities) and meteorological variables were also measured at MLO. MLO is a nearly ideal location for making such atmospheric electricity measurements: it is located at the centre of the island of Mauna Loa, far from urban coastal sources of pollution, and severe weather is relatively rare. Also, MLO's high elevation places it generally well above the exchange layer (the lowest layer of the atmosphere which is most subject to turbulence and mixing).[36] Thus the air above MLO is less subject to variations due to local atmospheric fluctuations.

1960–61 and 1977–1982 MLO J_z data extending into the northern hemisphere winter months were visually inspected for calibration problems, and data segments of sufficiently high quality and quantity were selected for the analysis.

Date	DlyAveRatio	ΔVAI
1/1/1964	0.885	7.421
1/2/1964	0.930	-0.834
1/3/1964	1.110	-7.852
1/4/1964	1.003	2.431
1/5/1964	0.956	7.574

Lag = – 1 day

Date	DlyAveRatio	ΔVAI
1/1/1964	0.885	7.421
1/2/1964	0.930	-0.834
1/3/1964	1.110	-7.852
1/4/1964	1.003	2.431
1/5/1964	0.956	7.574

Lag = 0 days

Date	DlyAveRatio	ΔVAI
1/1/1964	0.885	7.421
1/2/1964	0.930	-0.834
1/3/1964	1.110	-7.852
1/4/1964	1.003	2.431
1/5/1964	0.956	7.574

Lag = +1 day

Figure 7. Simulated data set illustrating the pairing of values of *DlyAveRatio* (the proxy for daily average high-latitude values of J_z) with values of ΔVAI for lag values of –1, 0, and +1 days.

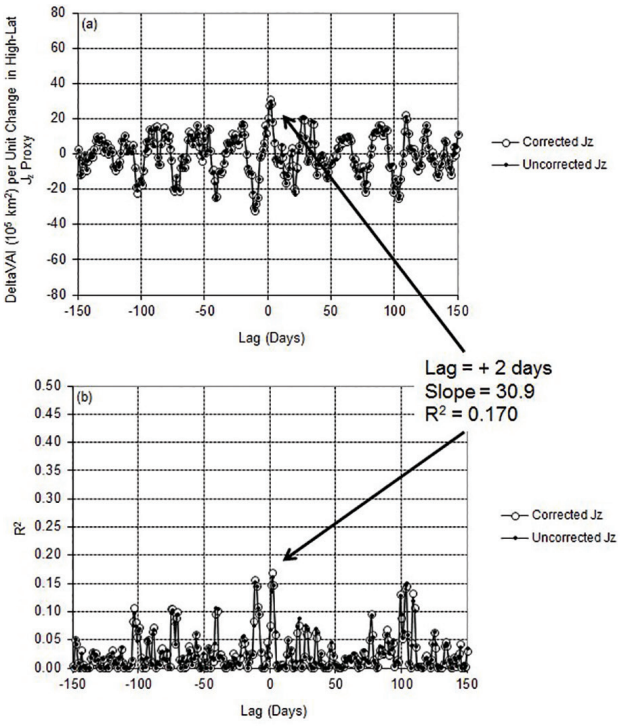

Figure 8. (a) Slope and (b) R^2 values (as a function of lag) resulting when the 106 1977–1982 proxy values for daily average November–March high-latitude J_z are used in regression analysis with anomalies in the 500 hPa 60–80° N VAI (after figure 5 in Hebert *et al.*[21]). Both the maximum positive slope and R^2 values (for both corrected and uncorrected J_z values) occur at a lag of +2 days. Text inset indicates the peak R^2 value (and accompanying slope value) obtained using the 'corrected' J_z data.

MLO J_z values experience a pronounced daily (or *diurnal*) variation,[33] and this was taken into account when obtaining values of the proxy (designated as *DlyAveRatio*) for daily average values of high latitude J_z. An attempt was made to reduce the 'noise' in the J_z data due to variations in atmospheric conductivity above the station and variations in wind speed and direction. Wind speed corrections were made to both the 1960–1961 and 1977–1982 J_z data sets, but conductivity corrections could only be made to the 1960–1961 J_z data, as the poor quality of the 1977–1982 conductivity data prevented such conductivity corrections from being made.

Daily average values of J_z are dependent upon daily average values of V_i, which in turn are dependent upon thunderstorm activity in all 24 time zones. In order to obtain the best possible proxy values, no value of *DlyAveRatio* was used in the analysis unless it was calculated with at least 21 hourly J_z values.

There was a change in the instrumentation used to measure J_z after 1961. The resulting calibration challenges were circumvented by analyzing the 1960–1961 and 1977–1982 data sets separately. However, the same procedure was used for both analyses.

More detailed explanations of the procedures are presented in a Ph.D. dissertation[37] and a recent paper.[21]

MLO regression results

Linear regressions of ΔVAI versus *DlyAveRatio* were performed for the 1960–1961 and 1977–1982 data sets; i.e. ΔVAI values for a given period were plotted against their corresponding *DlyAveRatio* values. However, it is possible that a peak VAI response to changes in J_z might be 'delayed' for a number of days; i.e. the VAI response might 'lag' somewhat behind a change in J_z. For this reason, linear regressions were performed for 'lag' values extending from –150 to +150 days (figure 7). For each lag value, both a slope (regression coefficient) and an R^2 value were calculated. One expects VAI responses to increased

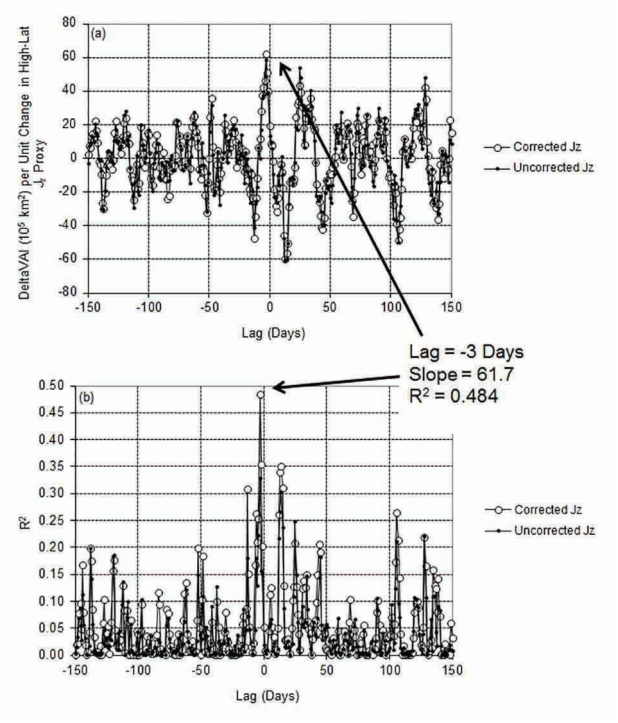

Figure 9. (a) Slope and (b) R^2 values (as a function of lag) resulting when the 32 1960–1961 proxy values for daily average November–March high-latitude J_z are used in regression analysis with anomalies in the 500 hPa 60–80° N VAI (after figure 6 in Hebert *et al.*[21]). Both the maximum positive slope and R^2 values (for both corrected and uncorrected J_z values) occur at a lag of −3 days. This slope is also larger in magnitude than any other slope value (positive or negative) within the 301-day interval. Text inset indicates the peak R^2 value (and accompanying slope value) obtained using the 'corrected' J_z data.

J_z to be characterized by (relatively) large positive slopes and R^2 values.

The 1977–1982 regression was performed using VAI values calculated from a combination of the older ERA 40 data (horizontal spatial resolution of 2.5º × 2.5º) and the newer ERA Interim data (horizontal spatial resolution of 1.5º × 1.5º). These data sets were archived by the European Centre for Medium-Range Forecasts as of April 2013.[38] The newer ERA Interim data only extended back to 1979. In order to obtain the best possible data for the regressions, the ERA Interim values were used for the 1979–1982 interval, and the ERA 40 values (after 'scaling' to 'match' the ERA Interim VAI values) were used for the 1977–1978 interval. The 1960–1961 regression used the 'scaled' ERA 40 values. Clear signals were obtained only when ΔVAI values were calculated using 500 hPa values for the 60–80° north latitude band. Slope and R^2 values for each of the 301 lag values were calculated using both the J_z data which had not been corrected for wind speed and

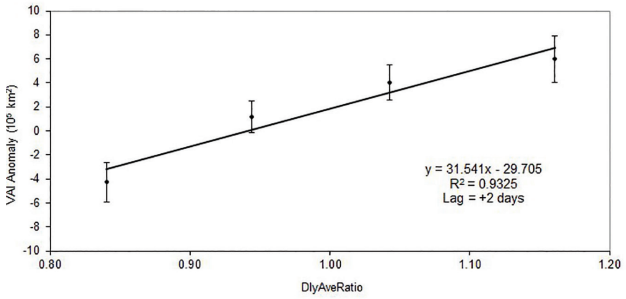

Figure 10. 500 hPa 60-80° N VAI response (at a lag of +2 days) for the four 1977–1982 winters (after binning of the data) to the 'corrected' high-latitude J_z proxy (After Figure 8 in Hebert *et al.*[21]). Error bars are +/-1 standard error on the mean.

conductivity variations, as well as the J_z data which *had* been corrected for these variations ('uncorrected' versus 'corrected'). The results are shown in figures 8 and 9.

In both cases, the very largest R^2 values occurred within 3 days of a lag of zero, regardless of whether 'corrected' or 'uncorrected' J_z values were used in the analysis. For both cases, these peak R^2 values were accompanied by the very largest positive regression coefficients (slope values). For the 1960–1961 'corrected' J_z data, this peak (positive) slope value was also the very largest magnitude regression coefficient (whether positive or negative) for the entire 301-day interval.

A statistically rigorous regression requires that the errors in the dependent variable be independent of one another, and this was not always the case: since the two regressions used *DlyAveRatio* values which were often calculated from J_z data on consecutive days, the errors in the corresponding ΔVAI values were not always independent (due to 'persistence' in the VAI values). A more rigorous estimate of the VAI response to J_z changes was obtained by 'binning' both the values of the dependent and independent variables, so that values which were adjacent to one another in time were generally placed in separate bins. The 1977–1982 period had sufficient data to re-perform the regression (for a lag of +2 days, using the 'corrected' J_z data) after placing the data in 4 separate bins. The results are shown in figure 10. An analysis-of-variance (ANOVA) test showed that this result was statistically significant at better than the 95% confidence level: there is less than 1 chance in 20 that the true slope (for a lag of +2 days) was actually zero.

Discussion

That, for two independent data sets, the peak positive VAI response occurred within 3 days of a lag of zero, would seem to provide support for Tinsley's hypothesis. However, these results also suggest a number of issues which should be addressed.

First, the much higher peak R^2 value for the 1960–1961 regression (using the 'corrected' J_z data) was likely due to a combination of the smaller number of available data points (a smaller number of data points favours larger R^2 values) and the fact that both wind speed *and* conductivity corrections were performed on the 1960–1961 J_z data (note from Figure 9b the roughly 50% increase in the peak R^2 value at the lag of –3 days that resulted from the corrections).

Second, is the peak 1960–1961 winter response at a small *negative* lag value inconsistent with the hypothesis? After all, if changes in J_z are *causing* changes in cyclonic intensity/vorticity, should not the responses occur at non-negative lag values? Yes, but it should be remembered that these are not ideal data sets. Noise in the data and persistence (autocorrelation) in the VAI (and possibly the small number of data points available for the 1960–1961 regression) likely resulted in this peak response being shifted to a small negative lag value. Furthermore, before the higher resolution ERA Interim data became available, these regressions had already been performed using only the older ERA 40 VAI values. The results were very similar to those shown in figures 8 and 9. As one might expect, only the magnitudes of the slope values were changed for the 1960–1961 regression (the peak slope value at the lag of –3 days was 47.7 units, rather than 61.7 units). The 1977–1982 regression yielded a peak response at a lag of +3 days, rather than the +2 days reported here. As in the case reported here, this R^2 value of 0.180 (calculated using 'corrected' J_z values) was the very largest for the 301-day interval, and the accompanying regression coefficient of 28.8 units was the very largest positive slope value for the interval (although a negative slope of about –29 units at a lag of –10 days was slightly larger in magnitude). Hence, the quality of the data used to calculate the VAI values can 'shift' the location of the peak response.

Atmospheric electricity data measurements are no longer being made at Mauna Loa Observatory, and no existing measurements of J_z from other atmospheric electricity stations are of sufficient quality and quantity to be used in such an analysis. Hence it is currently not possible to perform other regression analyses of changes in J_z with changes in the VAI (or with other meteorological variables). However, fair-weather values of the vertical surface electric field E_z are often used as rough proxy values for the global ionospheric potential V_i. Since V_i modulates J_z via eq. 1, it is hoped that future regressions performed using high-quality electric field data may also show a VAI response to V_i, helping to provide more clarity on this issue.

Concluding remarks

This cyclonic intensification is not predicted by Svensmark's IMN mechanism, since the IMN mechanism does not involve J_z.

When discussing the existence of a possible CMAS effect within the context of a discussion of 'global warming', an obvious question is: would a CMAS effect result in net cooling or heating? The answer to that question is not immediately obvious. The CMAS effect results in increased cloud cover and clouds with smaller average droplet sizes.[5] One might expect this to have a cooling effect, particularly at low latitudes (which receive larger amounts of incident sunlight), since greater numbers of low-latitude clouds (as well as low-latitude clouds with smaller average droplet sizes) would tend to reflect more sunlight back into space. However, it should also be remembered that cloud *albedo* (the fraction of incident sunlight reflected by clouds) also depends upon other factors besides just droplet size.[39] Moreover, the CMAS effect depends upon J_z, which in turn depends upon *other* factors, such as V_i and local ionisation rates and aerosol contents. Finally, it should also be remembered that an increase in cloud cover at one latitude could conceivably be accompanied by a *decrease* in cloud cover at another latitude.[6] Hence it is not immediately clear whether the CMAS effect would have a net heating or cooling effect.

However, the CMAS effect could result in an improved understanding of cloud microphysics. As acknowledged by the IPCC 4th Assessment Report, clouds are a major source of uncertainty in climatological models, as the amplitude and sign of cloud feedbacks are uncertain.[40] Thus a better understanding of cloud microphysics is critical in order to make an accurate assessment of the size of possible anthropogenic contributions to global warming. If the CMAS effect is real, then the failure of current models to take this effect into account will obviously be a source of error in such model predictions.

Finally, the CMAS mechanism may also help to explain the severity of European winters during the Maunder Minimum, the coldest part of the 'Little Ice Age' (and a period of extremely low solar activity), as well as some recent very cold European winters. It is hoped that this topic may be addressed in a future paper.

References

1. In recent years, the somewhat ambiguous description 'climate change' has been used more and more frequently. Of course, 'climate change' is harder to confirm (or falsify) than 'global warming'.
2. Oard, M.J., *The Frozen Record*, Institute for Creation Research, Santee, CA, pp. 123–132, 2005.
3. Carslaw, K.S., Harrison, R.G. and Kirkby, J., Cosmic rays, clouds, and climate, *Science* **298**:1732–1737, 2002.
4. In the interest of full disclosure, Tinsley was my Ph.D. advisor, and it should be noted that he does not share the editorial views of this journal.
5. Hebert, L., Two possible mechanisms linking cosmic rays to weather and climate, *J. Creation* **27**(2):91–98, 2013.
6. Hebert, L., Apparent difficulties with a CMAS cosmic ray–weather/climate link, *J. Creation* **27**(3):93–97, 2013.
7. Due to the interaction of the solar wind with the earth's magnetic field, high-latitude potentials are superimposed upon this global ionospheric potential. Outside the polar caps, however, the ionosphere may be thought of as an equipotential surface with electric potential V_i.
8. Tinsley, B.A., The global atmospheric electric circuit and its effects on cloud microphysics, *Rep. Prog. Phys*. **71**(066801):1–31, 2008.
9. Tinsley, B.A., Burns, G.B. and Zhou, L., The role of the global electric circuit in solar and internal forcing of clouds and climate, *J. Adv. Space Res*. **40**:1126–1139, 2007.
10. Williams, E.R. and Heckman, S.J., The local diurnal variation of cloud electrification and the global diurnal variation of negative charge on the earth, *J. Geophys. Res*. **98**(D3):5221–5234, 1993.
11. Bering, E.A. III, Few, A.A. and Benbrook, J.R., The global electric circuit, *Physics Today* **51**(10):24–30, 1998.
12. Tinsley *et al*., ref. 9, p. 1126.
13. Pruppacher, H.R. and Klett, J.D. *Microphysics of Clouds and Precipitation*, 2nd edn, Kluwer Academic, Dordrecht, The Netherlands, p. 802, 1997.
14. Pruppacher and Klett, ref. 13, p. 711.
15. Mason, B.J., *The Physics of Clouds*, 2nd edn, Clarendon Press, Oxford, p. 63, 1971.
16. Zhou, L., Tinsley, B.A. and Plemmons, A., Scavenging in weakly electrified saturated and subsaturated clouds, treating aerosol particles and droplets as conducting spheres, *J. Geophys. Res*. **114**:D18201, 2009.
17. Tinsley, B.A., Electric charge modulation of aerosol scavenging in clouds: rate coefficients with Monte Carlo simulation of diffusion, *J. Geophys. Res*. **115**:D23211, 2010.
18. Tinsley, B.A. and Deen, G.W., Apparent tropospheric response to MeV-GeV particle flux variations: a connection via electrofreezing of supercooled water in high-level clouds? *J. Geophys. Res*. **96**(D12):22283–22296, 1991.
19. Kirkland, M.W. and Tinsley, B.A., Are stratospheric aerosols the missing link between tropospheric vorticity and Earth transits of the heliospheric current sheet? *J. Geophys. Res*. **101**(D23):29689–29699, 1996.
20. Gringel, W., Rosen, J.M. and Hofmann, D.J., Electrical structure from 0 to 30 kilometers; in: *The Earth's Electrical Environment*, National Academy Press, Washington, D.C., pp. 166–182, 1986.
21. Hebert, L. III, Tinsley, B.A. and Zhou, L., Global electric circuit modulation of winter cyclone vorticity in the northern high latitudes, *J. Adv. Space Res*. **50**(6):806–818, 2012.
22. Pruppacher and Klett, ref. 13, p. 327.
23. Rosenfeld, D., Lohmann, U., Raga, G.B. *et al*., Flood or drought: how do aerosols affect precipitation? *Science* **321**:1309–1313, 2008.
24. *Baroclinic* cyclones tend to form along fronts, boundaries between air masses of different temperature and density, en.wikipedia.org/wiki/Extratropical_cyclone, as at 22 February 2013.
25. Weather Online website, weatheronline.co.uk/reports/wxfacts/The-Polar-low—-the-arctic-hurricane.htm, as at 24 April 2012.
26. Griffiths, D.J., *Introduction to Electrodynamics*, 2nd edn, Prentice-Hall, Englewood Cliffs, NJ, p. 22, 1989.
27. Holton, J.R., *An Introduction to Dynamic Meteorology*, 1st edn, Academic Press, New York, p. 65, 1972.
28. Technically, this curl is a vector that is 'dotted' into the local vertical unit vector (the unit vector perpendicular to the earth's surface) in order to obtain a simple positive or negative number for the vertical component of the vorticity.
29. This counter-clockwise rotation in the northern hemisphere is due to the well-known 'Coriolis Effect'.
30. Gringel *et al*., ref. 20, p. 167.
31. This may be due in part to the different geographies of the northern and southern hemispheres. The northern hemisphere has much more land mass, and the temperature contrast between the relatively cold land masses and the warm oceans is conducive to cyclone formation. Hence one might expect CMAS-induced cyclone intensification to be greatest in the northern hemisphere.
32. For the northern hemisphere, it is defined to be the surface area (in km^2) over which the absolute vorticity is greater than 20×10^{-5} s^{-1} plus the area over which the absolute vorticity exceeds 24×10^{-5} s^{-1}. See Roberts, W.O. and Olson, R.H., Geomagnetic storms and wintertime 300-mb trough development in the North Pacific-North America area, *J. Atmos. Sci*. **30**:135–140, 1973.
33. Cobb, W.E. and Phillips, B.B., Atmospheric electric measurements at Mauna Loa Observatory, Weather Bureau, U.S. Dept. of Commerce, Technical Paper No. 46, 1962.
34. Engfer, D.W. and Tinsley, B.A., An investigation of short-term solar wind modulation of atmospheric electricity at Mauna Loa Observatory, *J. Atmos. Solar Terr. Phys*. **61**, 943–953, 1999.
35. This assumes that both locations are outside the magnetic polar caps, where complications due to the interaction of the solar wind with the earth's magnetic field result in additional potential patterns being superimposed on the global ionospheric potential. Even within the magnetic polar caps, these superimposed potential patterns are very small in comparison to the global ionospheric potential V_i.
36. Price, S. and Pales, J.C., Mauna Loa Observatory: The First Five Years, *Mon. Wea. Rev*. **91**:665–680, 1963.
37. Hebert, L., Atmospheric Electricity Data from Mauna Loa Observatory: Additional Support for a Global Electric Circuit–Weather Connection? *Ph.D. dissertation*, University of Texas at Dallas, 2011.
38. www.ecmwf.int/products/data/archive/index.html.
39. Lutgens, F.K., Tarbuck, E.J. and Tasa, D., *The Atmosphere: An Introduction to Meteorology*, 11th edn, Prentice Hall, New York, p. 55, 2010.
40. IPCC Fourth Assessment Report: Climate Change 2007, Working Group I: The Physical Science Basis, Section 1.5.2, 'Model Clouds and Climate Sensitivity', ipcc.ch/publications_and_data/ar4/wg1/en/ch1s1-5-2.html, as at 25 April 2012.
41. Holzer, T.E., *Solar System Plasma Physics*, vol. I, Elsevier Science Publishers, North-Holland, p. 103, 1979.
42. Smith, E.J., *Rev. Geophys. Space Phys*. (American Geophysical Union) **17**:610, 1979.
43. Griffiths, ref. 26, figure 1.19, p. 23.

Jake Hebert *earned a B.S. from Lamar University, an M.S. from Texas A&M University, and a Ph.D. from the University of Texas at Dallas (all degrees in physics). He studied optics at Texas A&M and was a 1995-96 Dean's Graduate Fellow. His Ph.D. research involved a study of the possible connection between fair-weather atmospheric electricity and weather and climate. He has taught at both the high school and university levels and became a research associate at the Institute for Creation Research in 2011, where his research interests include climates before and after the Flood, cosmology, and general apologetics.*